An online substructure identification method for local structural health monitoring

Jilin Hou[1]‡, **Łukasz Jankowski**[2] **and Jinping Ou**[1,3]

[1] School of Civil Engineering, Dalian University of Technology, Dalian 116024, P. R. of China

[2] Institute of Fundamental Technological Research (IPPT PAN), ul. Pawińskiego 5b, 02-106 Warsaw, Poland

[3] School of Civil Engineering, Harbin Institute of Technology, Harbin 150090, P. R. of China

E-mail: `hou.jilin@hotmail.com`

Abstract. This paper proposes a substructure isolation method, which uses time series of measured local response for online monitoring of substructures. The proposed monitoring process consists of two key steps: construction of the isolated substructure, and its identification. Isolated substructure is an independent virtual structure, which is numerically isolated from the global structure by placing virtual supports on the interface. First, the isolated substructure is constructed by a specific linear combination of time series of its measured local responses. Then, the isolated substructure is identified using its local natural frequencies extracted from the combined responses. The substructure is assumed to be linear; the outside part of the global structure can have any characteristics. The method has no requirements on the initial state of the structure, and so the process can be carried out repetitively for online monitoring. Online isolation and monitoring is illustrated in a numerical example with a frame model, and then verified in an experiment of a cantilever beam.

Smart Mater. Struct. **22** (2013) 095017 doi:10.1088/0964-1726/22/9/095017
(http://iopscience.iop.org/0964-1726/22/9/095017)

‡ Corresponding author: hou.jilin@hotmail.com

1. Introduction

In the last decade, Structural Health Monitoring (SHM) has become an important and widely researched field. New monitoring techniques are being developed and increasingly wider applied for safety and reliability of civil engineering structures. The applications often focus on large and specialized structures. Such complex structures are difficult to be monitored globally using typical approaches of low frequency structural health monitoring (SHM) due to several inherent reasons, such as poor accuracy of global parametric models, poor sensitivity of the global response to local damages, poor numerical convergence, practical limitations concerning sensor number and placement, unknown excitations sources and boundary conditions, etc. However, in many practical applications only small local substructures are crucial and need monitoring, which suggests that there is a practical need for substructuring methodologies that would allow typical global SHM approaches to be applied locally. Such small substructures feature much fewer structural parameters or unknown factors and can be identified with only a few sensors, which makes local modeling and analysis much more feasible in comparison to global approaches.

Damages of substructures can be detected by a comparison before and after damage of local sensitive information, such as local model, strain, or dynamic response [1, 2, 3]. However, these methods sometimes detect only the presence of damage. Because the substructure is a local part of the global structure, accuracy of local identification can be readily compromised by concurrent changes of other parts of the structure. Most of the present substructuring methods are based on the equation of motion of the substructure. The response in time domain is widely used with techniques such as Kalman filter [4, 5], auto-regressive and moving average model (ARMAX) [6, 7] or the least squares method [8]. For example, Tee et al. [5] perform the identification at the substructure level using an observer/Kalman filter method based either on the equation of state or the equation of motion. Further, in 2009 [9], they use a method called Condensed Model Identification and Recovery to condense and then retrieve local parameters in order to avoid the complete measurement. The ARMAX model was used in 2011 by Xing and Mita [7] to localize the damage of any storey in a shear structure building. In the same year, Wang et al. [8] develop an online identification method of hysteretic parameters of the restoring force using the least squares method in pseudo-dynamic tests. In all these methods, the interface of the substructure is the key factor in identification. The "quasi-static displacement" approach was adopted by Koh et al. [10] and Wang et al. [11] to simplify the equation of motion of the substructure; a genetic algorithm (GA) is employed then for optimization. In 2012, Trinh and Koh [12] compute the interface velocity and displacement from the measured interface acceleration using a numerical integration scheme, and then utilize a multi-feature GA method to estimate the parameters of the substructure. Law and Young [13] use a two-step optimization procedure, in which the finite element model of a damaged substructure and the interface forces are alternately updated in each iteration. Hou et al. propose in [14, 15] a substructure isolation method (SIM), which first numerically constrains the interface responses to zero and then isolates the substructure into an independent and virtual isolated substructure. Such an isolated substructure can be flexibly identified using any of the existing methods aimed originally at global identification. Some references perform the identification in frequency domain. Yuen and Katafygiotis [16] present in 2006 a bayesian frequency-domain approach based on the FFT of measured noisy responses. In 2010, Zhang et al. [17] identify each storey of a shear structure using the Cross Power Spectral Density (CPSD).

In many practical applications, the crucial substructures need to be monitored in real time. The Substructure Isolation Method proposed in [14, 15] required zero initial state of the substructure and all the loads to be deliberately applied transient excitations, which ruled out applications for online identification. This paper drops the assumption of zero initial conditions and uses the isolation methodology with time series (SIM-TS) of locally measured responses to operational excitations, which extends the application area of the Substructure Isolation Method and makes it capable of online tracking of substructural damage. The present literature often uses least-square estimation [8, 18] or adaptive extended Kalman filtering [19] to track the structural damage online in time domain. The proposed SIM-TS is different from other methods, as it consists of two steps. First, the substructure is numerically isolated from the global structure into an independent virtual structure, of which the responses are constructed by a combination of the measured responses in time domain. Then, the identification of the isolated substructure is performed based on its local natural frequencies identified from the constructed responses. It is well known that natural frequencies represent the most basic dynamic information of a structure, and they are widely used in damage identification [20, 21, 22]. Finally, the procedure can be performed repeatedly for the purpose of online identification.

This paper is structured as follows: section 2 provides an overview of the required sensors and measurements. Section 3 gives the derivation of the substructure isolation using time series. Local identification is discussed in section 4. In section 5, a numerical frame structure is utilized to introduce the application of the method. In section 6, a beam experiment is performed to verify the proposed method.

2. Instrumentation

2.1. Sensors

The substructure is virtually isolated from the global structure by placing virtual supports in all its interface degrees of freedom (DOFs). In practice, these supports are implemented by I_B physical *interface sensors* (the corresponding response is x_i, $i = 1, \ldots, I_\mathrm{B}$), which are placed and used for the purpose of isolation only. Besides, there are I_S *internal sensors* (the corresponding response is y_i, $i = 1, \ldots, I_\mathrm{S}$) which are placed inside the substructure in order to measure its response.

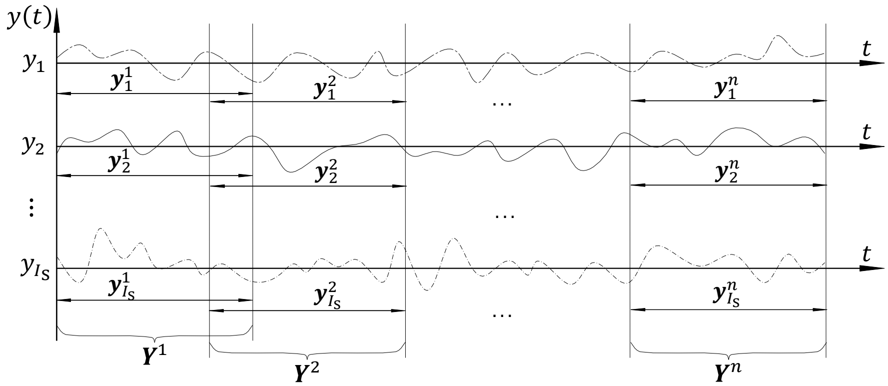

Figure 1. Responses of the internal sensors, time series $\boldsymbol{y}_i^n$ and their ordering into the vectors $\boldsymbol{Y}^n$.

2.2. Excitations

The proposed isolation approach uses no intentionally applied excitations inside the substructure. It is assumed that the main sources of excitation are located on the interface or outside the substructure, that is the substructure is excited through its interface rather than by internal excitations. As a result, all the considered sensors measure the response of the substructure to its interface excitation which corresponds to the actual excitations of the outside structure such as wind, vehicle traffic, running engines, any other operational excitation, or modal hammer, etc.

2.3. Measurement time series

It is assumed that the discrete responses of the interface and internal sensors are measured online. The measurements are denoted respectively by $\{x_i(t_k)\}$ and $\{y_i(t_k)\}$, where $k = 1, 2, \ldots$ indexes the time steps. By using successive and possibly overlapping time sections, the measurements are divided into the corresponding time series, each of length K,

$$\begin{aligned} \boldsymbol{x}_i^n &:= \{x_i^n(t_k^n)\}\,, \\ \boldsymbol{y}_i^n &:= \{y_i^n(t_k^n)\}\,, \end{aligned} \tag{1}$$

where n is the number of the time section, $k = 1, \ldots, K$ indexes the time steps anew within each time section, and $t_1^n < t_1^{n+1}$ for all n. In each time section, the readings of all the interface sensors $\boldsymbol{x}_i^n$, $i = 1, \ldots, I_\mathrm{B}$, are combined into a single interface response vector $\boldsymbol{X}^n$, which is of length $I_\mathrm{B}K$. In a similar way, the readings of all the internal sensors $\boldsymbol{y}_i^n$, $i = 1, \ldots, I_\mathrm{S}$, are combined into a single internal response vector $\boldsymbol{Y}^n$ of length $I_\mathrm{S}K$. For the internal sensors, this process is illustrated in figure 1.

3. Isolation of the substructure

The substructure is assumed to be linear. The isolation process is equivalent to altering the responses of the internal sensors (using a linear combination with coefficients dependent on the interface response) in such a way that the result equals their responses *as if* they were placed in a physically isolated substructure, that is in a substructure with physical supports in the interface DOFs instead of the interface sensors. The isolation process is carried out numerically, so that the constructed response is the response of a *virtual* isolated substructure rather than of a real physical substructure. The response constructed this way is used to extract local modal properties of the substructure for the purpose of local health monitoring.

3.1. The combined response

Assume that the time series (1) are extracted from the measurements and combined into the response vectors $\boldsymbol{X}^n$ and $\boldsymbol{Y}^n$ for $n = 1, \ldots, N+1$. Consider the following combined response vectors:

$$\boldsymbol{C}_{\mathrm{X}}^{N+1} := \boldsymbol{X}^{N+1} + \sum_{n=1}^{N} \alpha_n \boldsymbol{X}^n = \boldsymbol{X}^{N+1} + \boldsymbol{X}^{1:N}\boldsymbol{\alpha}, \tag{2}$$

$$\boldsymbol{C}_{\mathrm{Y}}^{N+1} := \boldsymbol{Y}^{N+1} + \sum_{n=1}^{N} \alpha_n \boldsymbol{Y}^n = \boldsymbol{Y}^{N+1} + \boldsymbol{Y}^{1:N}\boldsymbol{\alpha}, \tag{3}$$

where the vector $\boldsymbol{\alpha}$ collects the combination coefficients α_n, and $\boldsymbol{X}^{1:N}$ and $\boldsymbol{Y}^{1:N}$ are matrices composed respectively of column vectors $\boldsymbol{X}^1$ to $\boldsymbol{X}^N$ and $\boldsymbol{Y}^1$ to $\boldsymbol{Y}^N$. If the substructure is assumed linear, the combined response vectors $\boldsymbol{C}_{\mathrm{X}}^{N+1}$ and $\boldsymbol{C}_{\mathrm{Y}}^{N+1}$ are its valid responses (that is certain solutions to its equation of motion) and can be thus used for monitoring. Moreover, if the matrix $\boldsymbol{X}^{1:N}$ is of full row rank, for which a necessary condition is $N \geq I_{\mathrm{B}}K$, or more specifically, if it is not row rank-deficient [23], then the combination coefficients can be selected in such a way that the combined interface response vanishes,

$$\boldsymbol{C}_{\mathrm{X}}^{N+1} = \boldsymbol{X}^{N+1} + \boldsymbol{X}^{1:N}\boldsymbol{\alpha} = \boldsymbol{0}, \tag{4}$$

$$\boldsymbol{\alpha} := \boldsymbol{\alpha}^{N+1} = -\left[\boldsymbol{X}^{1:N}\right]^{\star} \boldsymbol{X}^{N+1}, \tag{5}$$

where the superscript "$\star$" denotes the (regularized) pseudo-inverse of a matrix. In such a case, the corresponding combined vector of the internal response,

$$\begin{aligned} \boldsymbol{C}_{\mathrm{Y}}^{N+1} &= \boldsymbol{Y}^{N+1} + \boldsymbol{Y}^{1:N}\boldsymbol{\alpha}^{N+1} \\ &= \boldsymbol{Y}^{N+1} - \boldsymbol{Y}^{1:N}\left[\boldsymbol{X}^{1:N}\right]^{\star}\boldsymbol{X}^{N+1}, \end{aligned} \tag{6}$$

is the response of the *isolated substructure*, that is the response of the actual substructure, but as if it was physically isolated from the outside structure. The isolation is achieved numerically by combining the responses of the interface sensors to zero.

Theoretically, there is no limitation on the type of the excitation, which can be random, continuous, impact-type, operational, etc. However, in order to obtain a reliable solution of (4), the response matrix $\boldsymbol{X}^{1:N}$ should not be rank-deficient. Consequently, excitations with a wide frequency spectrum are recommended, so that the response conveys more information about the dynamics of the substructure. In addition, since (4) is a numerically ill-conditioned equation, the amplitude of the excitation should be large enough to ensure a high signal-to-noise ratio.

3.2. Equation of motion and the isolated substructure

The equation of motion of the substructure, including its interface DOFs, can be stated as follows:

$$\begin{aligned}\begin{bmatrix} \boldsymbol{f}_{\mathrm{b}}(t) \\ \boldsymbol{f}_{\mathrm{s}}(t) \end{bmatrix} = \begin{bmatrix} \boldsymbol{M}_{\mathrm{bb}} & \boldsymbol{M}_{\mathrm{bs}} \\ \boldsymbol{M}_{\mathrm{sb}} & \boldsymbol{M}_{\mathrm{ss}} \end{bmatrix} \begin{bmatrix} \ddot{\boldsymbol{z}}_{\mathrm{b}}(t) \\ \ddot{\boldsymbol{z}}_{\mathrm{s}}(t) \end{bmatrix} + \begin{bmatrix} \boldsymbol{C}_{\mathrm{bb}} & \boldsymbol{C}_{\mathrm{bs}} \\ \boldsymbol{C}_{\mathrm{sb}} & \boldsymbol{C}_{\mathrm{ss}} \end{bmatrix} \begin{bmatrix} \dot{\boldsymbol{z}}_{\mathrm{b}}(t) \\ \dot{\boldsymbol{z}}_{\mathrm{s}}(t) \end{bmatrix} \\ + \begin{bmatrix} \boldsymbol{K}_{\mathrm{bb}} & \boldsymbol{K}_{\mathrm{bs}} \\ \boldsymbol{K}_{\mathrm{sb}} & \boldsymbol{K}_{\mathrm{ss}} \end{bmatrix} \begin{bmatrix} \boldsymbol{z}_{\mathrm{b}}(t) \\ \boldsymbol{z}_{\mathrm{s}}(t) \end{bmatrix}\end{aligned} \tag{7}$$

where the subscript "b" relates to the DOFs of the substructural interface (boundary), the subscript "s" denotes the DOFs inside the substructure, and $\boldsymbol{z}_{\square}(t)$, $\dot{\boldsymbol{z}}_{\square}(t)$, $\ddot{\boldsymbol{z}}_{\square}(t)$ with the respective subscripts stand for the displacement, velocity and acceleration of the respective substructural DOFs. The substructure is excited by $\boldsymbol{f}_{\mathrm{b}}(t)$ in its interface DOFs and by $\boldsymbol{f}_{\mathrm{s}}(t)$ in its internal DOFs; the latter excitation will be later assumed to vanish.

The substructure is assumed to be linear, and so its linearly combined responses in (4) and (6) are its valid responses to the respectively combined excitations, that is discretized solutions to the equation of motion. According to the type of the interface sensors, three kinds of the interface response can be measured, combined into $\boldsymbol{C}_{\mathrm{X}}^{N+1}$ and made vanishing by selecting the combination coefficients as in (5):

(i) If the *displacements* are combined to zero, then $\boldsymbol{z}_{\mathrm{b}}(t) = \boldsymbol{0}$ and obviously also the velocities and accelerations in the interface DOFs vanish, $\dot{\boldsymbol{z}}_{\mathrm{b}}(t) = \ddot{\boldsymbol{z}}_{\mathrm{b}}(t) = \boldsymbol{0}$.

(ii) If the *velocities* are combined to zero, then $\dot{\boldsymbol{z}}_{\mathrm{b}}(t) = \boldsymbol{0}$ and so also $\ddot{\boldsymbol{z}}_{\mathrm{b}}(t) = \boldsymbol{0}$, but the displacement is a constant that might be different from zero, $\boldsymbol{z}_{\mathrm{b}}(t) = \boldsymbol{x}_0$.

(iii) Finally, if the *accelerations* are combined to zero, then $\ddot{\boldsymbol{z}}_{\mathrm{b}}(t) = \boldsymbol{0}$, but the velocity is a constant that might be different from zero, $\dot{\boldsymbol{z}}_{\mathrm{b}}(t) = \boldsymbol{v}_0$. Accordingly, the displacement in the interface DOFs is a linear function of time,

$$\boldsymbol{z}_{\mathrm{b}}(t) = \boldsymbol{x}_0 + \boldsymbol{v}_0 t. \tag{8}$$

Among these three cases, the third is the most general and includes the two previous cases: the second case corresponds to $\boldsymbol{v}_0 = \boldsymbol{0}$, while the first case requires $\boldsymbol{x}_0 = \boldsymbol{0}$ and $\boldsymbol{v}_0 = \boldsymbol{0}$. If the general combined solution (8) is substituted into (7), then the equation of motion in the internal DOFs is simplified to

$$\begin{aligned}&\boldsymbol{C}_{\mathrm{fs}}^{N+1}(t) - \boldsymbol{K}_{\mathrm{sb}}\boldsymbol{v}_0 t - (\boldsymbol{K}_{\mathrm{sb}}\boldsymbol{x}_0 + \boldsymbol{C}_{\mathrm{bs}}\boldsymbol{v}_0) \\ &\qquad = \boldsymbol{M}_{\mathrm{ss}}\ddot{\boldsymbol{z}}_{\mathrm{s}}(t) + \boldsymbol{C}_{\mathrm{ss}}\dot{\boldsymbol{z}}_{\mathrm{s}}(t) + \boldsymbol{K}_{\mathrm{ss}}\boldsymbol{z}_{\mathrm{s}}(t)\end{aligned} \tag{9}$$

where $\boldsymbol{C}_{\mathrm{fs}}^{N+1}(t)$ is the internal excitation of the substructure combined in the respective time sections using the same combination coefficient $\boldsymbol{\alpha}^{N+1}$ as in (5). The solution to (9) consists of two parts: a special solution and a general solution,

$$\boldsymbol{z}_{\mathrm{s}}(t) = \boldsymbol{z}_{\mathrm{s}}^{\star}(t) + \boldsymbol{z}_{\mathrm{s}}^{\#}(t). \tag{10}$$

The special solution $\boldsymbol{z}_{\mathrm{s}}^{\star}(t)$ to the linear excitation by the interface DOFs is also linear and can be obtained easily as

$$\begin{aligned}\boldsymbol{z}_{\mathrm{s}}^{\star}(t) = &-\boldsymbol{K}_{\mathrm{ss}}^{-1}\boldsymbol{K}_{\mathrm{sb}}\boldsymbol{v}_0 t \\ &+\boldsymbol{K}_{\mathrm{ss}}^{-1}\left(\boldsymbol{C}_{\mathrm{ss}}\boldsymbol{K}_{\mathrm{ss}}^{-1}\boldsymbol{K}_{\mathrm{sb}}\boldsymbol{v}_0 - \boldsymbol{K}_{\mathrm{sb}}\boldsymbol{x}_0 - \boldsymbol{C}_{\mathrm{bs}}\boldsymbol{v}_0\right),\end{aligned} \tag{11}$$

while the general solution $\boldsymbol{z}_{\mathrm{s}}^{\#}$ stands for any response of the substructure to the combined internal excitation,

$$\boldsymbol{C}_{\mathrm{fs}}^{N+1}(t) = \boldsymbol{M}_{\mathrm{ss}}\ddot{\boldsymbol{z}}_{\mathrm{s}}^{\#}(t) + \boldsymbol{C}_{\mathrm{ss}}\dot{\boldsymbol{z}}_{\mathrm{s}}^{\#}(t) + \boldsymbol{K}_{\mathrm{ss}}\boldsymbol{z}_{\mathrm{s}}^{\#}(t). \tag{12}$$

All the parameters in (12), such as the mass, damping and stiffness matrices, $\boldsymbol{M}_{\mathrm{ss}}$, $\boldsymbol{C}_{\mathrm{ss}}$ and $\boldsymbol{K}_{\mathrm{ss}}$, the combined excitation $\boldsymbol{C}_{\mathrm{fs}}^{N+1}(t)$ or the response $\boldsymbol{z}_{\mathrm{s}}^{\#}(t)$, are related only to the substructure, so that there are no influences of the other parts of the global structure. As a result, equation (12) is an equation of motion of an independent system. Such a virtually constructed, independent system is called the *isolated substructure*. Its parameters, $\boldsymbol{M}_{\mathrm{ss}}$, $\boldsymbol{C}_{\mathrm{ss}}$ and $\boldsymbol{K}_{\mathrm{ss}}$, can be estimated by an analysis of the output $\boldsymbol{z}_{\mathrm{s}}^{\#}(t)$ and the input $\boldsymbol{C}_{\mathrm{fs}}^{N+1}(t)$. In this paper, no internal excitation is assumed, $\boldsymbol{C}_{\mathrm{fs}}^{N+1}(t) = \mathbf{0}$, and so the general solution $\boldsymbol{z}_{\mathrm{s}}^{\#}(t)$ is the *free response* of the isolated substructure, which can be directly used to identify its local modal properties for the purposes of identification of substructural parameters and local damage identification.

3.3. The combined response vs. the free response of the isolated substructure

In practice, combination (6) of the experimentally measured responses yields a discretized version of either displacements $\boldsymbol{z}_{\mathrm{s}}(t)$, velocities $\dot{\boldsymbol{z}}_{\mathrm{s}}(t)$ or accelerations $\ddot{\boldsymbol{z}}_{\mathrm{s}}(t)$, depending on the type of the internal sensors. According to (10) and (11), the combined response corresponds thus to one of the following

$$\begin{aligned}\boldsymbol{z}_{\mathrm{s}}(t) =& \boldsymbol{z}_{\mathrm{s}}^{\#}(t) - \boldsymbol{K}_{\mathrm{ss}}^{-1}\boldsymbol{K}_{\mathrm{sb}}\boldsymbol{v}_0 t \\ &+ \boldsymbol{K}_{\mathrm{ss}}^{-1}\left(\boldsymbol{C}_{\mathrm{ss}}\boldsymbol{K}_{\mathrm{ss}}^{-1}\boldsymbol{K}_{\mathrm{sb}}\boldsymbol{v}_0 - \boldsymbol{K}_{\mathrm{sb}}\boldsymbol{x}_0 - \boldsymbol{C}_{\mathrm{bs}}\boldsymbol{v}_0\right),\end{aligned} \tag{13}$$

$$\dot{\boldsymbol{z}}_{\mathrm{s}}(t) = \dot{\boldsymbol{z}}_{\mathrm{s}}^{\#}(t) - \boldsymbol{K}_{\mathrm{ss}}^{-1}\boldsymbol{K}_{\mathrm{sb}}\boldsymbol{v}_0, \tag{14}$$

$$\ddot{\boldsymbol{z}}_{\mathrm{s}}(t) = \ddot{\boldsymbol{z}}_{\mathrm{s}}^{\#}(t), \tag{15}$$

where either $\boldsymbol{v}_0$ or both $\boldsymbol{v}_0$, $\boldsymbol{x}_0$ can vanish, depending on the type of the interface sensors. Notice that only the free response of the isolated substructure (the general solution) $\boldsymbol{z}_{\mathrm{s}}^{\#}(t)$, $\dot{\boldsymbol{z}}_{\mathrm{s}}^{\#}(t)$ or $\ddot{\boldsymbol{z}}_{\mathrm{s}}^{\#}(t)$, provides useful information about the substructure and is of interest here. The difference between the combined response obtained from the experimental data and the local free response can either vanish, be constant or linear, which depends on the types of the interface and internal sensors as summarized in Table 1.

3.4. Selection of the time series

The process of extracting the time series from the measurement data depends on certain important parameters, such as the sampling frequency f_{s}, the length of the time series K,

Table 1. The difference between the combined response $\boldsymbol{C}_{\mathrm{Y}}^{N+1}$ and the general solution (the free response in case of no internal excitations) of the isolated substructure.

	Measured internal response		
Measured interface response	Displacement	Velocity	Acceleration
Displacement	zero	zero	zero
Velocity	constant	zero	zero
Acceleration	linear	constant	zero

the number of the time series N, and the time delay between the adjacent time series $\Delta t = t_{n+1}^{i} - t_{n}^{i}$. Accuracy of the constructed free responses and natural frequencies of the isolated substructure depends on their numerical values.

Theoretically, the sampling frequency should satisfy the relation $f_{\mathrm{s}} \geq 2f_{\mathrm{m}}$ and the length of the time series K should satisfy $K > 2f_{\mathrm{s}}/f_1$, where f_{m} denotes the largest considered natural frequency of the isolated substructure and f_1 denotes its first natural frequency. The number of the time series N should be large enough to allow the combination of I_{B} interface sensors to vanish in K time steps, for which a necessary condition is $N \geq I_{\mathrm{B}}K$. For convenience, it will be usually assumed that the time delay between the adjacent time series Δt is constant and equals one or two time steps.

4. Online local health monitoring

4.1. Modal identification of the substructure

The isolated substructure is a virtually constructed, independent structure that satisfies the equation of motion (12). Such a structure can be identified and monitored by an analysis of its constructed local response (6) and the accordingly combined internal excitation. Basically, any classical, well-researched identification method can be used for this purpose, see [24, 25]; this is unlike other substructuring methods, which simultaneously have to take into account also the interface forces that couple the substructure to the global structure, and which thus need dedicated, non-standard identification approaches.

Here, no internal excitation is used, so that the constructed response is the *free response* of the isolated substructure, perhaps with a constant bias or a linear trend, see table 1. Such a response can be directly used to identify local modal properties. The most basic dynamic information of a structure is represented by its natural frequencies, and damage identification methods based on natural frequencies are simple and fast [20, 21, 22, 25, 26, 27]. Moreover, local natural frequencies of the isolated substructure can be reasonably expected to be much more sensitive to its local damage than the global natural frequencies. Therefore, this paper uses natural frequencies of the isolated substructure for the purpose of local monitoring. As a result, a very limited number of internal sensors is required for substructural identification. On the other hand, for the purpose of isolating the substructure, all interface DOFs should be instrumented.

Local natural frequencies can be identified from the constructed free response of the isolated substructure by the Eigensystem Realization Algorithm (ERA, [28]). Denote the ith identified local natural frequency by ω_i^{M}, and the corresponding natural frequency computed using a Finite Element (FE) model of the isolated substructure by $\omega_i^{\mathrm{FEM}}(\boldsymbol{\mu})$. Let the vector $\boldsymbol{\mu}$ collect the unknown damage parameters of the substructure; it is identified here by minimizing the following objective function:

$$\Delta(\boldsymbol{\mu}) := \sum_i \left| \frac{\omega_i^{\mathrm{FEM}}(\boldsymbol{\mu}) - \omega_i^{\mathrm{M}}}{\omega_i^{\mathrm{M}}} \right|^2. \tag{16}$$

In order to improve the efficiency of the optimization, sensitivities of the natural frequencies $\omega_i^{\mathrm{FEM}}(\boldsymbol{\mu})$ can be computed in each iteration [26, 27] and used with any standard gradient-based optimization approach.

4.2. Online monitoring

The proposed method can be used for online substructure identification due to its unique features, which can be listed as follows:

- There is no limitation on the excitation outside the substructure, which can be random excitation or operational loads, impact-type excitation, or any other general excitation. This enables the method to be widely used in real applications.
- There is no limitation on the initial state of the structure. The time series (1) can be selected beginning from any moment of the measured response.
- The substructure can be identified quickly and efficiently using the identified natural frequencies of the isolated substructure.

Because of the above characteristics, the time series can be extracted online, stage by stage, and the identification results in each stage will express the current damage state of the substructure. Figure 2 shows the flow chart of the online identification.

5. Numerical example

A 2-floor frame with two spans (Figure 3) is taken as an example to test the proposed online substructuring method. The frame contains six pillars and four beams, which are numbered as shown in Figure 3. Each floor is 0.6 m high, and the length of each span is 0.6 m. The density is 7850 kg/m^3, and Young's modulus is 210 GPa. The cross-section of all the pillars and beams is 6 mm $\times$ 50 mm. The first and the second order damping ratios are set as 1%. Table 2 lists the first 14 natural frequencies of the global frame. The second pillar in the first floor is chosen as the substructure to be virtually isolated and monitored online.

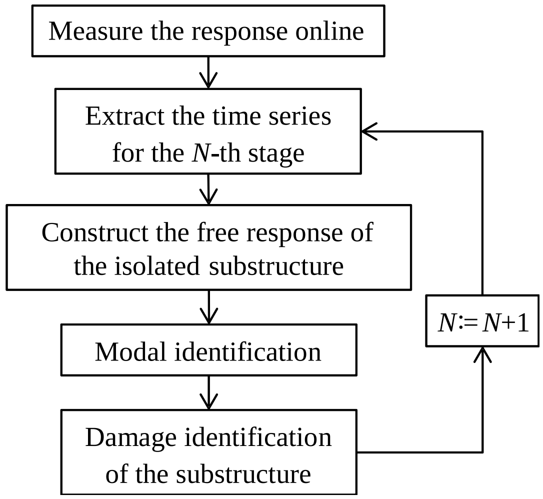

Figure 2. The flow chart of the online identification of the substructure.

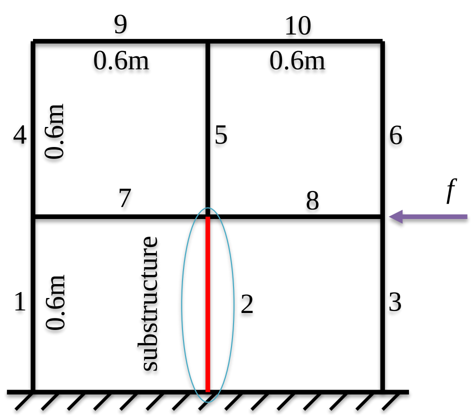

Figure 3. Numerical example: the frame structure.

Table 2. Numerical example: natural frequencies of the frame structure.

order	1	2	3	4	5	6	7
frequency [Hz]	5.74	18.22	42.55	52.09	58.04	69.05	70.73
order	8	9	10	11	12	13	14
frequency [Hz]	88.61	88.70	88.70	88.72	98.04	166.66	182.44

5.1. Isolation of the substructure

The exposed DOFs of the substructure interface (Figure 4a) are horizontal displacement u_1, axial displacement u_2, and rotation θ. Since the axial displacement is very small, only the horizontal displacement and the rotation are considered for isolation as the dominant interface DOFs. In a real application, a rotation is usually not easy to measure, while it is easy to obtain structural accelerations. In order to isolate the substructure using accelerations, a rigid horizontal massless element is introduced with one end fixed in the interface node and the other end free; it is marked with the dash line in Figure 4b. Let

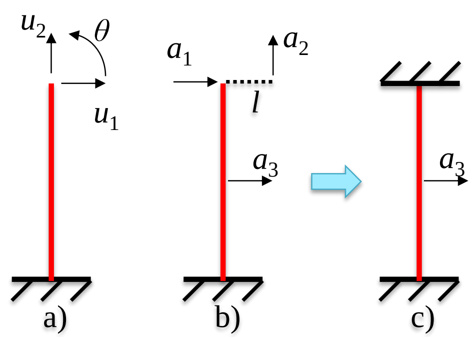

Figure 4. Numerical example: (a) interface of the substructure; (b) sensor placement; (c) isolated substructure.

a_2 denote the vertical acceleration of its free end, and it can be expressed in terms of the second derivatives of the axial displacement u_2 and the rotation θ,

$$\begin{aligned} a_1 &= \ddot{u}_1, \\ a_2 &= \ddot{u}_2 + \ddot{\theta} l, \end{aligned} \tag{17}$$

where $l = 60$ mm is the length of the rigid element. Besides a_2, accelerations at the other two positions also need to be measured: the interface horizontal acceleration a_1, and the horizontal acceleration a_3 in the middle of the substructure. If the interface acceleration responses a_1 and a_2 are combined to zero using the proposed method, they can be equivalently converted to virtual fixed supports. Then the substructure is separated from the global structure into an isolated substructure, see Figure 4c, and the acceleration response constructed with (6) at the position of a_3 can be used for local identification. The first natural frequency of the intact isolated substructure is 88.73 Hz.

5.2. Structural damage extents

Damage extent of each structural member is modeled in terms of its stiffness reduction,

$$\mu_i := \frac{\tilde{E}_i}{E_i}, \tag{18}$$

where E_i and $\tilde{E}_i$ denote respectively the original and reduced stiffness of the ith element. Assume that the damage extents of all elements can be changing with time and let the measurement time interval be 21 s. The damage extent $\mu_2(t)$ of the 2nd pillar (the substructure) is assumed to satisfy

$$\mu_2(t) := \begin{cases} 1 & \text{if } t \leq 7 \text{ s} \\ 0.8 & \text{if } 7 \text{ s} < t \leq 14 \text{ s} \\ 0.8 - 2(t-14)/35 & \text{if } 14 \text{ s} < t \leq 21 \text{ s} \end{cases} \tag{19}$$

Figure 5 plots the assumed time histories of the damage extents of all elements.

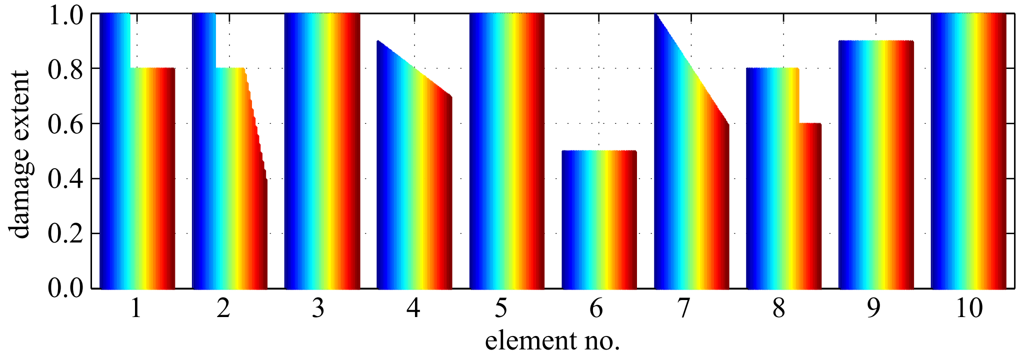

Figure 5. Numerical example: simulated damage extents of frame elements.

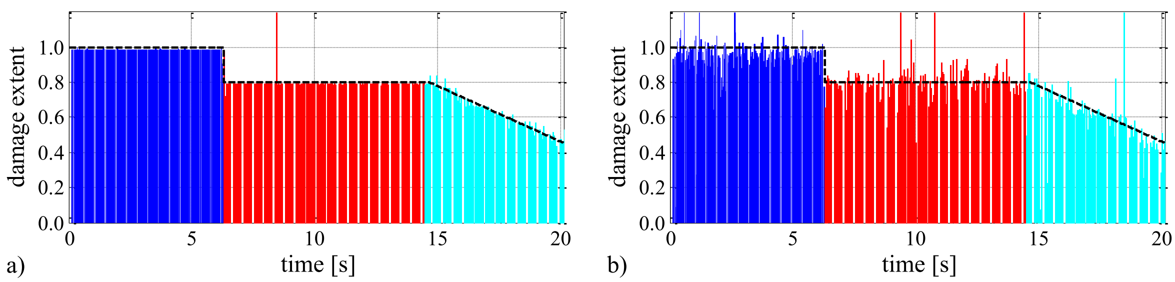

Figure 6. Numerical example, identified time histories of the substructural damage: (a) without measurement noise; (b) with simulated 5% Gaussian measurement noise.

5.3. Online identification of substructural damage

A white noise excitation is applied to the second floor at the position shown in Figure 3. Simulated acceleration responses a_1, a_2 and a_3 are collected at the positions shown in Figure 4. Section 3.4 lists certain parameters, which are important in the measurement process and in extraction of the time series. The sampling frequency f_s is 2000 Hz. The damage of the substructure is identified online every 0.025 s. The length K of the time series considered in each stage is 100 time steps, the number N of the time series is 220, and the time delay Δt between any two adjacent time series is one time step.

No excitation is applied inside the substructure, and so the free response of the isolated substructure is constructed in each stage of online identification. The local natural frequencies are identified by the Eigensystem Realization Algorithm (ERA, [28]). The substructure damage is then estimated by minimizing the objective function (16) using the identified and modeled natural frequency. First, the identification is based on the accurate simulated measurement data; the results are almost ideal, see Figure 6a. Then the measurements are contaminated with simulated Gaussian noise at 5% level; the results are plotted in Figure 6b, and their accuracy is still acceptable. The method is thus capable of detecting and tracking a damage that evolves in time, including sudden stepwise changes as well as slower gradual changes.

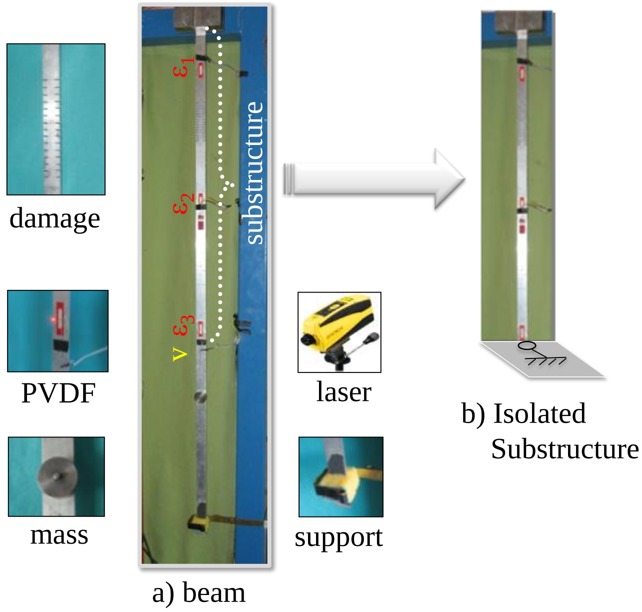

Figure 7. Experimental example, the cantilever beam with the instrumentation, and the isolated substructure.

6. Experimental example

6.1. Experimental setup

An aluminum cantilever beam is used for experimental verification of the proposed method, see Figure 7. The length of the beam is 136.15 cm, and the cross-section is 2.7 cm $\times$ 0.31 cm. Its Young's modulus is 70 GPa, and the density equals 2700 kg/m^3.

It is the part of the beam near the fixed end that is often important. The upper part is thus selected as the substructure to be locally monitored, see Figure 7a. The damage is modeled by cutting symmetrical notches along the beam near the fixed end on the length of 10.2 cm; the stiffness of the damaged segment is decreased to 42% of the original stiffness. It is difficult to have a varying damage extent during the sampling. Therefore, in the experiment, online monitoring of a changing structure is simulated by applying modifications outside the substructure. As a result, three different global beams that share the same substructure are successively tested, which in the following is referred to as the three phases of the experiment:

- *Beam B1,* which is the original beam (phase 1).
- *Beam B2,* which is the original beam with an additional mass attached outside the substructure (phase 2).
- *Beam B3,* which is the original beam with an additional "sponge support" used to fix its free end (phase 3).

In order to measure the response, three PVDF strain sensors are placed on the substructure, two inside and one on the interface, and a laser vibrometer is used to measure the interface transverse velocity. Figure 7a shows the placement of the sensors,

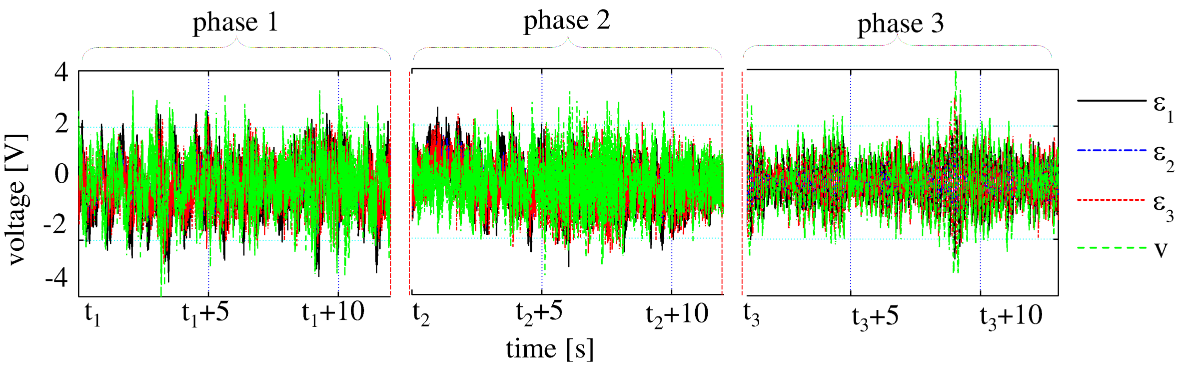

Figure 8. Experimental example, the response measured in the three phases.

which are denoted by ε_1, ε_2, ε_3, and v. When the responses of the interface sensors, that is strain ε_3 and velocity v, are combined to zeros, then they are effectively converted into virtual supports, which separate the substructure into an independent isolated substructure, which is shown in Figure 7b.

6.2. Excitation and responses

In the three phases of the experiment, the three versions of the beam are successively excited and measured. In each phase, several random hits with a simple hammer are applied outside the substructure and 12 s of the response is measured, see Figure 8, where the beginning of the ith phase is marked with t_i. The sampling frequency is 10 000 Hz.

6.3. Substructure isolation and identification

The damage of the substructure is identified online every 0.2 s, with a total of 50 identification in each phase and 150 identifications during the whole experiment. The length K of the time series considered for each identification is 2000 time steps, and the number N of the time series is 4000, while the time delay Δt between any two adjacent time series is one time step. The substructure is virtually isolated using linear combinations of the measured time series, which yields by (6) the free responses of the isolated substructure. The matrix $\boldsymbol{X}^{1:N}$ in (6) is a Toeplitz matrix, and due to the ill-conditioning of the deconvolution problem, the constructed responses are usually divergent near the end of the considered time interval. The initial 0.12 s of the constructed response is thus selected and used for modal identification. Examples of the free responses constructed in each phase are shown in Figure 9. These responses are used to identify the natural frequencies of the isolated substructure; the first seven of them are listed in Table 3 and compared with the accurate values obtained from numerical FE models of the intact and damaged isolated substructure. The natural frequencies identified in the three phases are close to each other and also to the natural frequencies of the damaged FE model, despite the fact that a different beam was used in each phase:

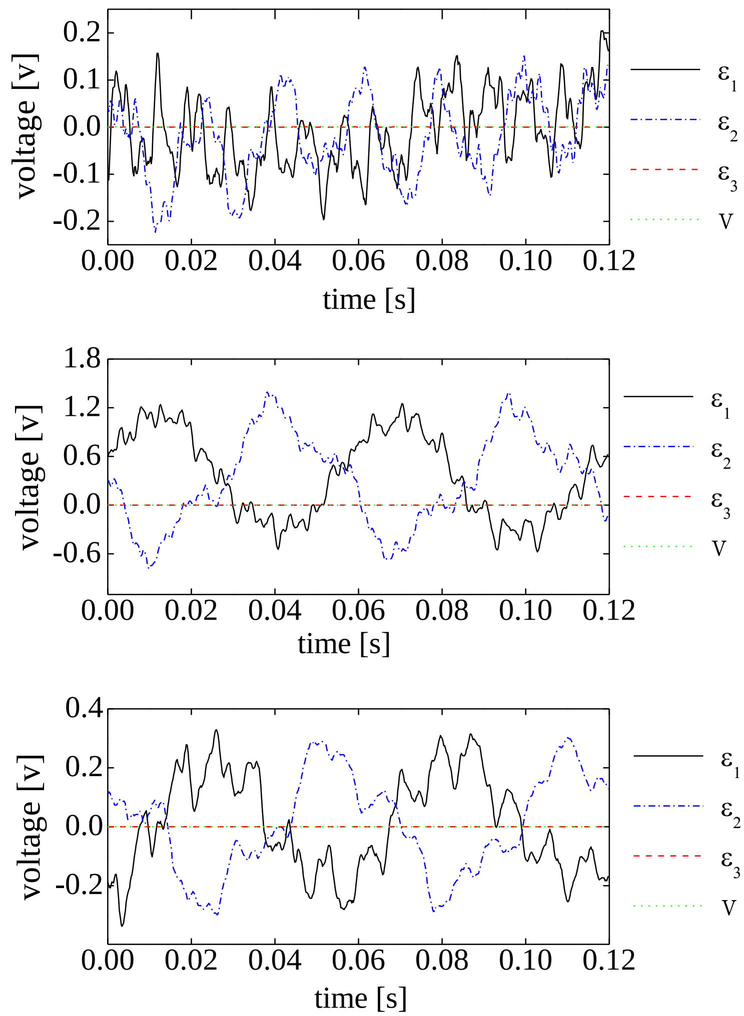

Figure 9. Experimental example, typical free responses constructed in (a) phase 1; (b) phase 2; (c) phase 3.

if the real substructures are the same, then the virtually isolated substructures are also the same, no matter if the outside structure is the same or not. In addition, it confirms the reliability of the constructed responses and the identified natural frequencies.

The substructure is divided into five segments, as shown in Figure 10. The second segment has the length of 10.2 cm and is damaged. The actual damage extents of the segments are thus [1.0 0.42 1.0 1.0 1.0] and remain the same in the three phases. The free responses of the isolated substructure are constructed a total of 150 times. Each time, the natural frequencies are found and used to identify the damage extents of the five segments by minimizing the objective function (16). The identification results are shown in Figure 11; the accuracy is acceptable. In the three phases, the substructure remains the same, but the outside components are different. Therefore, the results confirm that, using the proposed method, the identification of the substructure can be performed online even if the outside structure changes during the sampling.

Table 3. Experimental example: natural frequencies identified in each phase.

	FEM [Hz]		Identification [Hz]		
order	intact	damaged	phase 1	phase 2	phase 3
1	17.68	17.52	17.53	17.40	17.27
2	57.33	52.01	51.66	51.70	52.44
3	119.15	112.95	112.56	112.91	112.74
4	203.30	195.66	193.58	195.64	194.74
5	310.47	290.04	290.33	289.69	290.91
6	439.95	413.93	415.05	413.79	413.77
7	592.48	551.07	547.62	549.81	553.40

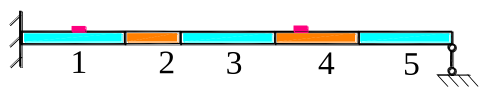

Figure 10. Experimental example, division of the substructure into five segments.

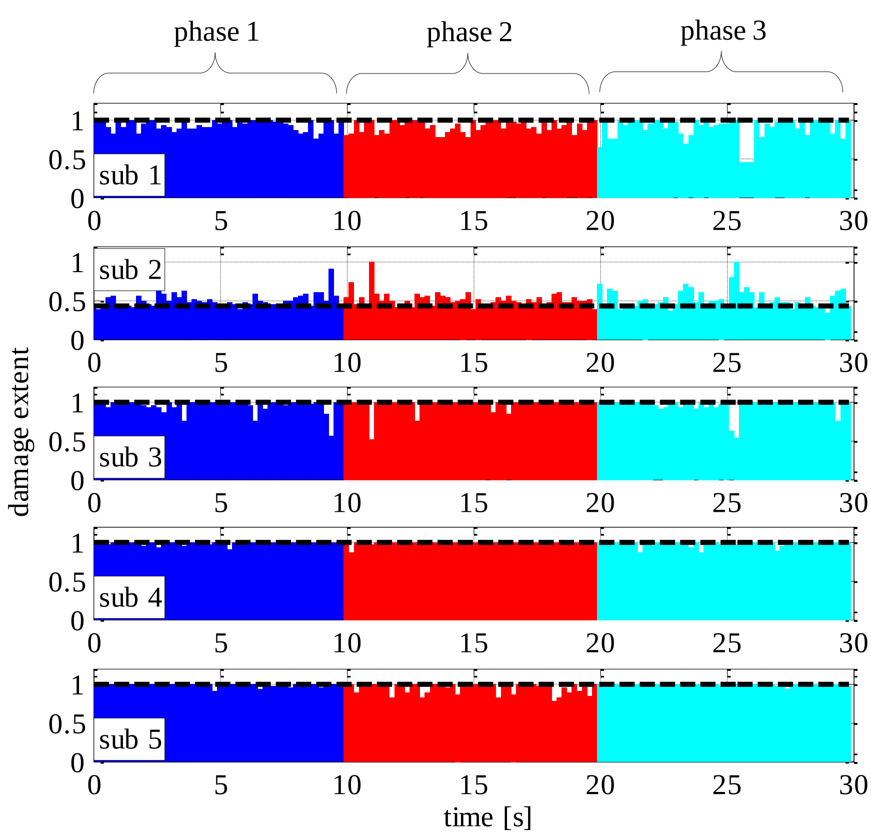

Figure 11. Experimental example, identified damage extents.

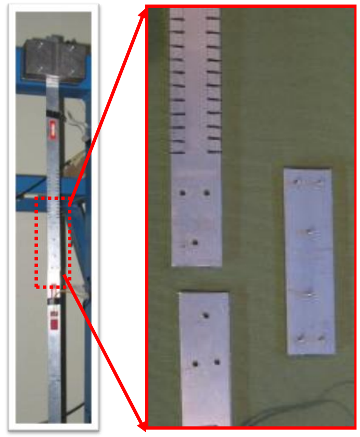

Figure 12. Experimental example, the screw connection in the substructure.

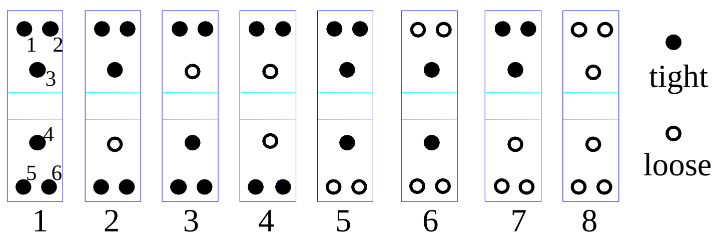

Figure 13. Experimental example, the eight cases of loose screws.

6.4. Detection of loose screws

In civil engineering, a screw is an important way of connecting elements. Loosening of screws can cause serious accidents. In this section, loose screws are detected using the proposed method. First, the beam mentioned above is cut into two parts in the middle of the substructure, and then the parts are connected again using a short aluminum plate and six screws as shown in Figure 12. According to which of these six screws are loose, eight cases shown in Figure 13 are designed and tested in the following. The dark color stands for the tight screws, while the light color stands for the loose screws. In the experiment, the loose screws are still in the beam.

In each case, hammer excitations are applied randomly outside the substructure. The response is measured and used to construct the free response of the isolated substructure. The natural frequencies are identified separately in each case and listed in Table 4. The results can be summarized as follows:

- In Case 1, all the screws are fixed well, so the isolated substructure is the stiffest, and the natural frequencies are correspondingly the largest.
- Although the number of the loose screws in Case 4 is the sum of that in Cases 2 and 3, the change of the natural frequencies in Case 4 (with respect to the intact Case 1) is not equal to the sum of the changes in Cases 2 and 3. The influence of the loose screws is thus not linear.

Table 4. Experimental example: the identified natural frequencies of the isolated substructure (in Hz).

Order	Case 1	Case 2	Case 3	Case 4	Case 5	Case 6	Case 7	Case 8
1	15.78	15.73	15.74	15.28	15.71	15.19	13.64	10.93
2	50.52	50.26	48.37	48.66	50.19	49.92	46.14	50.42
3	110.22	109.41	108.45	103.64	109.42	106.11	103.33	116.35
4	191.81	189.67	190.89	186.55	181.16	183.63	182.03	161.24
5	281.89	280.90	276.93	266.89	280.89	269.65	245.98	—
6	409.22	383.88	405.41	379.73	382.75	401.83	—	—
7	533.29	520.92	523.84	493.86	518.23	502.00	—	—

- The number of the loose screws in Cases 2 and 3 is the same, as well as in Cases 4 and 5, but the natural frequencies are different, because the positions of the loose screws are different.
- In Case 7, three underside screws are all loose, while in Case 8 all the screws are loose, so that the substructure is a nonlinear system. Theoretically, the substructure isolation method is not feasible for nonlinear substructures, and moreover, natural frequencies of a nonlinear system are time-varying. Here, although the identified natural frequencies in Cases 7 and 8 are only approximate, they still clearly reflect the decreased stiffness of the substructure. Loosening of almost all the screws significantly influences the dynamic characteristics of the beam, including a significant increase of damping. Consequently, the Eigensystem Realization Algorithm (ERA) cannot identify the highly damped higher order natural frequencies in Cases 7 and 8.

In short, the natural frequencies of the isolated substructure decrease as the number of the loose screws increases. The presence of loose screws and their number can be thus approximately detected using the proposed substructure isolation method. However, it is hard to locate exactly which screws are loose due to their complicated and nonlinear influence.

7. Conclusion

This paper extends the substructure isolation method to online local monitoring by using time series of the measured response. A numerical simulation of a frame model and a beam experiment are performed to verify the efficiency and accuracy of the proposed method. The substructural damage can be detected in real time. The conclusions are as follows:

- The initial state of the substructure can be non-zero, so that any section of the measured response can be selected for substructure identification. Such a free selection enables online identification.

- In order to construct a reliable response of the isolated substructure, it is recommended that the excitation has a wide frequency spectrum and an amplitude high enough to ensure a high signal-to-noise ratio.
- Local identification of the substructural damage is carried out efficiently using only the natural frequencies identified from the constructed free response. This simple identification increases the feasibility of the method for online applications.
- The type and the placement of interface sensors can be flexibly selected according to the demands of the application. However, the real-time performance and accuracy of the proposed method is better on simple substructures with a relatively small number of interface DOFs. These limitations are subjects of an ongoing research.

Acknowledgments

The authors gratefully acknowledge the support of the Major State Basic Research Development Program of China (973 Program)(2013CB036305), of National Science Foundation of China (NSFC) (51108057, 51108066), of the Fundamental Research Funds for the Central Universities(China) (DUT13LK13), of Special Financial Grant from the China Postdoctoral Science Foundation (2012T50255), and of the Project of National Key Technology R&D Program (China) (2011BAK02B01, 2011BAK02B03, 2006BAJ03B05). Financial support of the Polish National Science Centre Project "AIA" (DEC–2012/05/B/ST8/02971) and of Structural Funds in the Operational Programme–Innovative Economy (IE OP) financed from the European Regional Development Fund, Project "Modern material technologies in aerospace industry" (POIG.0101.02-00-015/08), is gratefully acknowledged.

References

[1] An Y and Ou J 2011 Experimental and numerical studies on model updating method of damage severity identification utilizing four cost functions *Structural Control and Health Monitoring* 20(1):107–120

[2] Bao Y, Li H, An Y and Ou J 2012 Dempster–Shafer evidence theory approach to structural damage detection *Structural Health Monitoring* 11(1):13–26

[3] Yun C-B and Bahng EY 2000 Substructural identification using neural networks *Computers and Structures* 77(1):41–52

[4] Oreta AWC and Tanabe T 1994 Element identification of member properties of framed structures *Journal of Structural Engineering* 120(7):1961–1976

[5] Tee KF, Koh CG and Quek ST 2005 Substructural first- and second-order model identification for structural damage assessment *Earthquake Engineering & Structural Dynamics* 34(15):1755–1775

[6] Yun C-B and Lee H-J 1997 Substructural identification for damage estimation of structures *Structural Safety*19(1):121–140

[7] Xing Z and Mita A 2012 A substructure approach to local damage detection of shear structure *Structural Control and Health Monitoring* 19(2):309–318

[8] Wang T, Wu B and Zhang J 2011 Online identification with least square method for pseudo-dynamic tests *Advanced Materials Research* 250–253:2455–2459

[9] Tee KF, Koh CG and Quek ST 2009 Numerical and Experimental Studies of a Substructural Identification Strategy *Structural Health Monitoring* 8(5):397–410

[10] Koh CG, Hong B and Liaw CY 2003 Substructural and progressive structural identification methods *Engineering Structures* 25(12):1551–1563

[11] Wang XJ, Koh CG and Zhang Z 2011 Damage identification based on strain and translational measurements with substructure approach *1st Middle East Conference on Smart Monitoring, Assessment and Rehabilitation of Civil Structure* Feb 8–10, Dubai, UAE

[12] Trinh TN and Koh CG 2012 An improved substructural identification strategy for large structural systems *Structural Control and Health Monitoring* 19(8):686–700

[13] Law SS and Yong D 2011 Substructure methods for structural condition assessment *Journal of Sound and Vibration* 330(15):3606–3619

[14] Hou J, Jankowski Ł and Ou J 2012 Experimental study of the substructure isolation method for local health monitoring *Structural Control and Health Monitoring* 19(4):491–510

[15] Hou J, Jankowski Ł and Ou J 2011 A substructure isolation method for local structural health monitoring *Structural Control and Health Monitoring* 18(6):601–618

[16] Yuen KV and Katafygiotis LS 2006 Substructure identification and health monitoring using noisy response measurements only *Computer-Aided Civil and Infrastructure Engineering* 21(4):280–291

[17] Zhang D and Johnson E A 2012 Substructure identification for shear structures: cross-power spectral density method *Smart Materials and Structures* 21 055006

[18] Yang J and Lin S 2004 On-line identification of non-linear hysteretic structures using an adaptive tracking technique *International Journal of Non-Linear Mechanics* 39(9):1481–1491

[19] Zhou L, Wu S and Yang JN 2008 Experimental study of an adaptive extended Kalman filter for structural damage identification *Journal of Infrastructure Systems* 1(14):42–51

[20] Salawu OS 1997 Detection of Structural Damage Through Changes in Frequency: A Review *Engineering Structures* 19(9):718–723

[21] Cawley P and Adams RD 1979 The locations of defects in structures from measurements of natural frequencies *Journal of Strain Analysis* 14(2):49–57

[22] Hassiotis S 2000 Identification of damage using natural frequencies and Markov parameters *Computers and Structures* 74(3):365–373

[23] Hansen PC 1987 *Rank-Deficient and Discrete Ill-Posed Problems: Numerical Aspects of Linear Inversion* (Philadelphia, PA: Society for Industrial and Applied Mathematics)

[24] Fan W and Qiao P 2011 Vibration-based Damage Identification Methods: A Review and Comparative Study *Structural Health Monitoring* 10(1):83–111

[25] Doebling SW, and Farrar CR and Prime MB 1998 A Summary Review of Vibration-Based Damage Identification Methods *The Shock and Vibration Digest* 30:91–105

[26] Fox R and Kapoor M 1968 Rates of Change of Eigenvalues and Eigenvectors *AIAA Journal* 6(12):2426–2429

[27] Nelson RB 1976 Simplified Calculation of Eigenvector Derivatives *AIAA Journal* 14(9):1201–1205

[28] Juang J-N and Pappa R 1985 An eigensystem realization algorithm for modal parameter identification and model reduction *Journal of Guidance, Control, and Dynamics* 8(5):620–627